Observation of quantum Griffiths singularity and ferromagnetism at the superconducting $LaAlO_3/SrTiO_3(110)$ interface

Shengchun Shen,[1] Ying Xing,[2,3] Pengjie Wang,[2] Haiwen Liu,[1] Hailong Fu,[2] Yangwei Zhang,[2] Lin He,[1] X. C. Xie,[2,4] Xi Lin,[2,4,*] Jiacai Nie,[1,†] and Jian Wang[2,4,‡]

[1]*Department of Physics, Beijing Normal University, Beijing 100875, People's Republic of China*

[2]*International Center for Quantum Materials, School of Physics, Peking University, Beijing 100871, People's Republic of China*

[3]*Beijing Key Laboratory of Optical Detection Technology for Oil and Gas, China University of Petroleum, Beijing 102249, China*

[4]*Collaborative Innovation Center of Quantum Matter, Beijing, 100871, People's Republic of China*

(Received 5 June 2016; published 25 October 2016)

Diverse phenomena emerge at the interface between band insulators $LaAlO_3$ and $SrTiO_3$, such as superconductivity and ferromagnetism, showing an opportunity for potential applications as well as contributing to fundamental research interests. Here, we report the superconductor-metal transition driven by a perpendicular magnetic field in superconducting two-dimensional electron gas formed at the $LaAlO_3/SrTiO_3(110)$ interface, which offers an appealing platform for quantum phase transition from a superconductor to a weakly localized metal. Interestingly, when approaching the quantum critical point, the dynamic critical exponent is not a constant but a diverging value, which is direct evidence of a quantum Griffiths singularity arising from quenched disorder at ultralow temperatures. Furthermore, the hysteretic property of magnetoresistance is observed at the $LaAlO_3/SrTiO_3(110)$ interface, which suggests the potential coexistence of superconductivity and ferromagnetism.

DOI: 10.1103/PhysRevB.94.144517

I. INTRODUCTION

Two-dimensional electron gas (2DEG) formed at the interface between two band insulators $LaAlO_3$ (LAO) and $SrTiO_3$ (STO) [1] exhibits many fascinating properties, such as superconductivity [2], magnetism [3], and their coexistence [2–6]. Historically, 2DEG has been a perfect system in which to study the quantum Hall effect, fractional quantum Hall effect, the charge density wave, and the transition between them by varying the charge density or magnetic field [7–10]. In 2DEG of LAO/STO(001), the quantum phase transition (QPT) is also an important topic, and the transition from a superconducting state to a weakly insulating state has been studied [11,12]. Most previous studies have focused on LAO/STO(001) due to feasible fabrication and polarization of the interface. Recently, controlled growth of pseudo-cubic-oriented and nonpolarized LAO/STO(110) interfaces has been successfully achieved, which makes related investigations possible [13–15].

Commonly, critical behavior depends only on the universality class of the transition, and not on microscopic details. However, quenched disorder can have profound effects on phase transitions and critical points [16–19], especially in QPTs [20–22]. If the average disorder strength diverges under coarse graining, the critical behavior shows the infinite-randomness quantum critical points (QCPs), where the conventional power-law scaling is replaced by activated scaling, namely, the quantum Griffiths singularity [23–25]. The quantum Griffiths singularity has been widely studied in theoretical works, but there is only limited experimental evidence in three-dimensional ferromagnetic metals [21,26]. Surprisingly, a recent unexpected observation exhibited the quantum Griffith singularity of a superconductor-metal transition (SMT) in three-monolayer-thick superconducting Ga films [27,28]. Whether or not the quantum Griffiths singularity is a universal scenario for QPTs in superconducting systems still remains a very interesting question. The verification of the quantum Griffiths singularity can help to identify the role of disorder in superconducting systems and hopefully may provide clues to a generalized theoretical framework for disordered QPTs.

Here, we report the observation of the quantum Griffiths singularity at the superconducting LAO/STO(110) interface. The QPT from a superconductor to a weakly insulating metal is driven by a perpendicular magnetic field. The conventional power-law scaling is replaced by activated scaling, and the dynamical exponent z diverges upon approaching the transition. An unconventional quantum critical behavior associated with the quantum Griffiths singularity is deduced and infinite-randomness quantum critical points are further concluded. Additional data with similar behaviors at back-gate voltages $V_G = 20$ V and 60 V are presented for a comprehensive understanding. In addition, the hysteretic magnetoresistance is observed, which indicates the existence of ferromagnetism at the LAO/STO(110) interface.

II. EXPERIMENTS

In total, 5 unit cells of LAO films were grown by pulsed laser deposition (PLD) (KrF, $\lambda = 248$ nm, laser fluence 1.5 J/cm^2, 1 Hz, at 750 °C, on top of treated (110)-STO substrates [see Fig. 7(b) in the Appendix]. Atomically flat (110)-STO surfaces were obtained after annealing at 1050 °C for 2 hours under oxygen atmosphere. Before deposition, the substrate was heated from room temperature to 750 °C in 0.1 mbar of O_2, and then the LAO layer was deposited in 10^{-5} mbar of O_2. After deposition, the sample was cooled in

*xilin@pku.edu.cn
†jcnie@bnu.edu.cn
‡jianwangphysics@pku.edu.cn

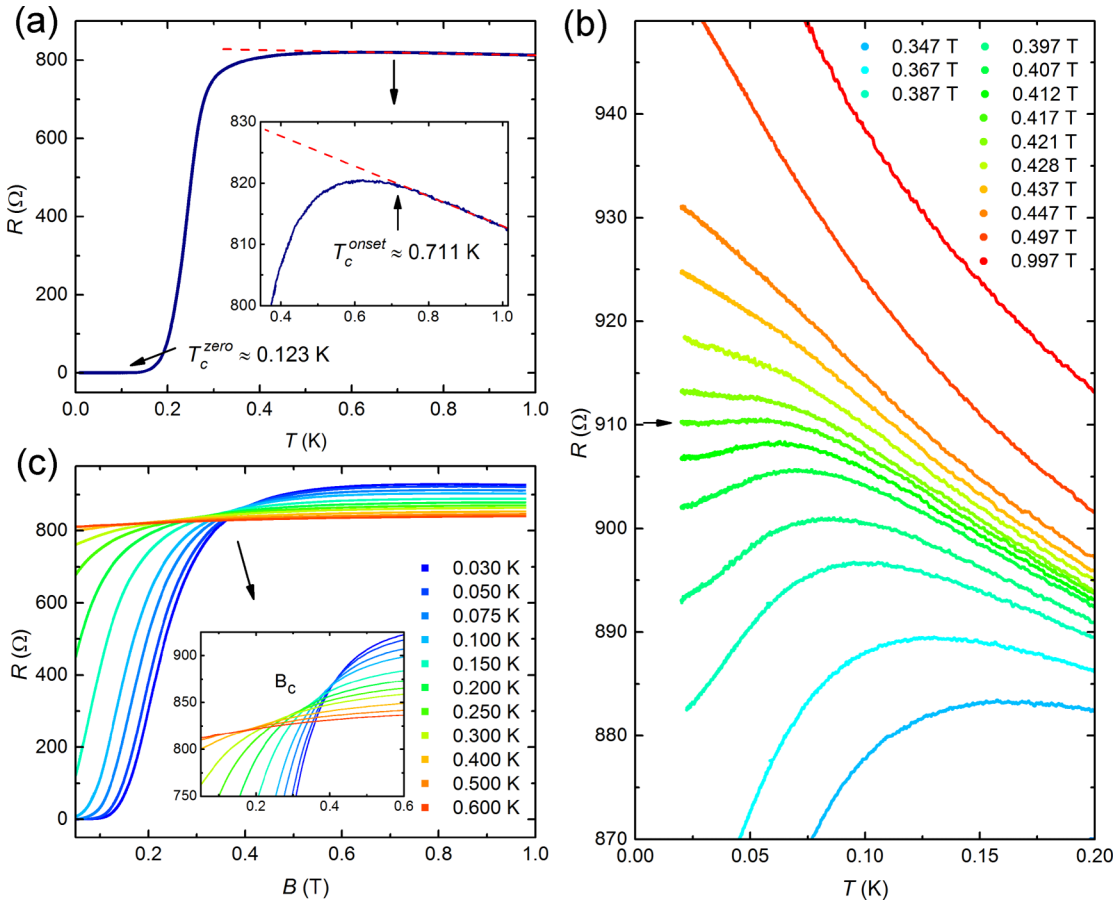

FIG. 1. The magnetic-field-driven superconductor-metal transition. (a) The temperature dependence of resistance at zero magnetic field. $T_c^{\rm zero}$ and $T_c^{\rm onset}$, marked by black arrow, are 0.123 K and 0.711 K, respectively. The inset shows the determination of $T_c^{\rm onset}$. (b) Isomagnetic $R(T)$ curves measured at different B. (c) Isotherm $R(B)$ curves measured at different T, where the inset shows the zoom-in view of the crossing region.

an oxygen-rich atmosphere to avoid the formation of oxygen vacancy. More details were described in Ref. [14].

For transport measurement, Al wires were attached to the interface by wedge bonding. A metallic back gate was evaporated and attached to the rear of the 500-μm-thick $SrTiO_3$ substrate. Leakage current was below 1 nA for a back-gate voltage of 60 V at low temperatures (<1 K). Standard four-probe resistance measurements were made with sufficiently low excitation current (50 nA at 6.47 Hz) to avoid any heating of the electrons at the lowest temperature. The samples were cooled in a dilution refrigerator MNK126-450 system (Leiden Cryogenics BV, base temperature <6 mK). A perpendicular magnetic field was applied to the sample surface. All the data for SMT were obtained for one direction of the field sweep. The magnetic field sweep rate was 1.35 mT/s for large-scale measurement of magnetoresistance [Fig. 1(c)] and 0.656 mT/s for detailed measurement of magnetoresistance [Fig. 2], respectively.

III. RESULTS AND DISCUSSION

Superconductivity and the SMT were found in our LAO/STO samples. As shown in Fig. 1(a), the temperature dependence of resistance at zero magnetic field reveals the interface is superconducting, with transition temperature $T_c^{\rm zero} \approx 0.123$ K and $T_c^{\rm onset} \approx 0.711$ K, respectively. $T_c^{\rm zero}$ is identified as the temperature at which the R drops beyond the measurement limit, while $T_c^{\rm onset}$ is identified as the temperature where $R(T)$ first deviates from its linear dependence at high temperature [see the inset of Fig. 1(a)]. With increasing magnetic field, the superconductivity is suppressed, and the system gradually becomes weakly insulating. The isomagnetics $R(T)$ show that resistance changes very slightly at the ultralow temperatures with a critical field (around 0.417 T) that separates two regimes, as shown in Fig. 1(b). As the signature of B-driven SMT, the magnetoresistance $R(B)$ curves measured at different temperatures cross each other around 0.385 T, as shown in Fig. 1(c). Previous studies have shown that a superconductor-insulator transition (SIT) occurs in the LAO/STO(001) system induced by magnetic field or charge density [11,12].

The crossing of the magnetoresistance isotherms happens in a well-distinguished region rather than at a single point in the magnetic field, as shown in Fig. 1(c). A similar crossing region was also observed in another LAO/STO(110) sample (see Fig. 11 in the Appendix). The crossing information allows a systematic investigation of the critical behavior, which was done through careful measurements of R versus B at temperatures ranging from 0.020 K to 0.650 K. As shown in Fig. 2, series of crossing points are observed. Crossing points

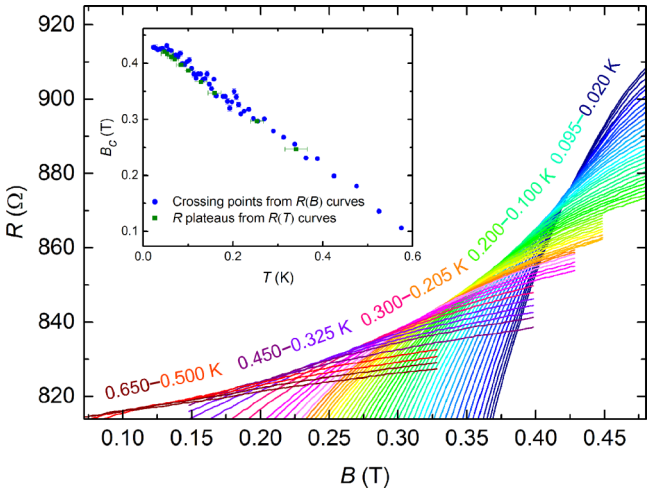

FIG. 2. The isotherms of magnetoresistance $R(B)$ from 0.020 K to 0.650 K. The sweep directions and rates are the same for all the curves. The inset shows the T dependence of corresponding B_c for crossing points (blue dots) of every two adjacent $R(B)$ curves, and the resistance plateaus (green squares) extracted from $R(T)$ curves.

of $R(B)$ isotherms at every two adjacent temperatures as a function of T are shown in the inset of Fig. 2 (blue dots), which form a roughly linear line. The R plateaus extracted from the $R(T)$ curves are shown as green squares, at which the dR/dT changes sign for a given magnetic field. The crossing points are consistent with R plateaus. In addition, we note that the crossing region of the magnetoresistance curves extends over a relatively wide range of magnetic fields and temperatures. This is reasonable since superconductivity emerges at relatively high temperature [$T_c^{\rm onset} \approx 0.711$ K; inset of Fig. 1(a)] in our LAO/STO(110) samples.

In order to gain more information about the phase transition, finite-size scaling (FSS) analysis of the critical regime is required. The resistance takes the scaling form [27,29–31],

$$R(B,T) = R_c f[(B - B_c)/T^{1/z\nu}], \qquad (1)$$

where R_c and B_c are the critical sheet resistance and the critical magnetic field, respectively, at which the transition occurs, $f[]$ is an arbitrary function of B and T with $f[0] = 1$, z is the dynamical critical exponent, and ν is the correlation length exponent. The scaling form is rewritten as $R(B,t)/R_c = f[(B - B_c)t]$, where $t = (T/T_0)^{-1/z\nu}$, which can be obtained by performing a numerical minimization between the curve $R(B,t)$ at a particular temperature T and the lowest temperature T_0 curve $R(B,t = 1)$. As shown in Fig. 2, every two adjacent R(B) curves cross at one point. In the FSS analysis, at least three curves are needed. Here, for the purpose of effective analysis, the small crossing region, formed by four adjacent $R(B)$ curves, is regarded approximately as one "critical" point. Figure 3(a) shows one representative group of isothermal curves with a "critical" point ($B_c = 0.427$ T, $R_c = 877.50\,\Omega$). The results of the FSS analysis show that the data collapse onto a bivalue curve, and the power-law dependence of t with temperature gives $z\nu = 3.37 \pm 0.50$ [Fig. 3(b)]. Nine representative groups with different temperature regions were selected (see Figs. 8 and 9 in the Appendix for the other eight groups), and series of $z\nu$ values, varying with decreasing temperature, were obtained. It has been reported [32] that FSS analysis can be applied in a restricted range of finite temperature for 2D superconductors under magnetic field, if considering the existence of inhomogeneities in the low-temperature phase.

By obtaining the $z\nu$ values in different ranges of temperature, we observed that $z\nu$ increases with decreasing temperature. It should be noted that $z\nu$ corresponds to a temperature region rather than a certain temperature. Figure 4 shows the magnetic field dependence of $z\nu$ values. In the high-temperature regime, $z\nu$ increases slowly with magnetic field, while $z\nu$ grows rapidly in the low-temperature regime. We fit the experimental $z\nu$ values in the low-temperature regions ($z\nu \geqslant 1$) as a function of B using the activated scaling law $z\nu \approx C|B - B_c^*|^{-\nu\psi}$, where C is constant, and ν and Ψ are the 2D infinite randomness critical exponents [33,34]; here, $\nu \approx 1.2$, and $\psi \approx 0.5$. The experimental results are in reasonable agreement with theoretical expectation (the blue line in Fig. 4, where $B_c^* = 0.428$ T), indicating infinite-randomness quantum critical points. With decreasing temperature, the effect of quenched disorder is enhanced, and the $z\nu$ value diverges when the critical point B_c^* is approached.

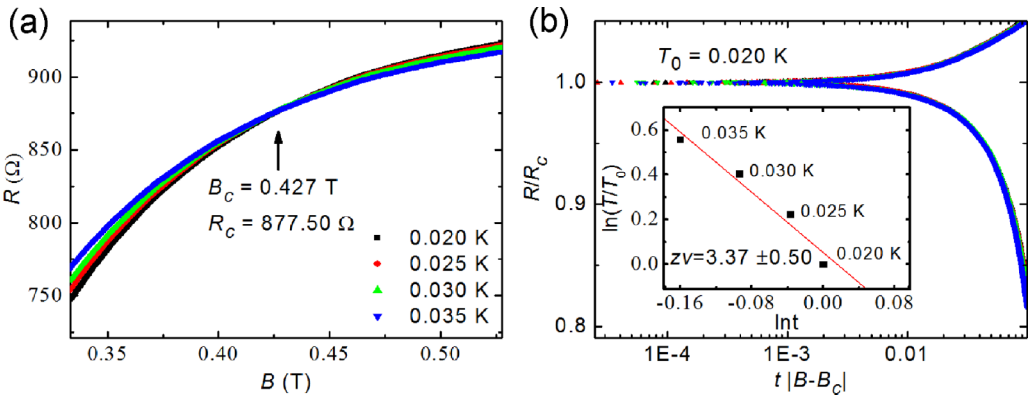

FIG. 3. Finite-size scaling analysis for one representative group. (a) The isotherms $R(B)$ close to the critical point in the lowest temperature region (0.020–0.035 K). The crossing region formed by four adjacent R(B) curves are denoted as one critical point ($B_c = 0.427$ T, $R_c = 877.50\,\Omega$). (b) Normalized R as a function of $t|B_c - B|$, where $t = (T/T_0)^{-1/z\nu}$. The insets show the power-law plot T dependence of scaling parameter t. The $z\nu$ value is obtained from the slope of the fitting line.

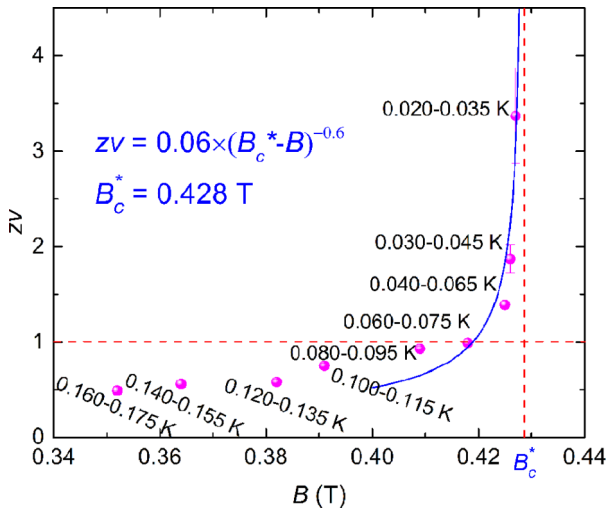

FIG. 4. The B dependence of critical exponent zv: activated scaling behavior. Magenta dots are zv values extracted from FSS analysis in different temperature regions. Blue line is the fitting by $zv = C(B_c^* - B)^{-0.6}$. Two red dash lines represent the constant value with $B_c^* = 0.428$ T and $zv = 1$, respectively.

Moreover, the properties of 2DEG at the LAO/STO interface can be tuned by a back-gate voltage. Figure 5(a) shows an $R(T)$ curve at zero magnetic field for $V_G = 20$ V with the superconducting transition temperature $T_c^{\text{zero}} \approx 0.109$ K and $T_c^{\text{onset}} \approx 0.696$ K, which are a little suppressed compared with those at zero back-gate voltage ($T_c^{\text{zero}} \approx 0.123$ K and $T_c^{\text{onset}} \approx 0.711$ K). The $R(B)$ isotherms show a crossing region around 0.365 T [Fig. 5(b)]. Further detailed measurements of magnetoresistance at the low-temperature range from 0.020 K to 0.300 K are shown in Fig. 5(c). Series of crossing points formed by every two adjacent magnetoresistance isotherms are observed. The extracted $B_c - T$ plot is shown in the inset of Fig. 5(c), which is analogous to the above case for $V_G = 0$ V (the inset of Fig. 2). The same FSS analysis described above was applied, and series of zv values were obtained. As shown in Fig. 5(d), the zv value diverges when temperature approaches zero, and theoretical fitting gives $B_c^* = 0.416$ T. The SMT for both $V_G = 20$ V and 60 V (Fig. 10 in the Appendix) displays behaviors that are also consistent with a quantum Griffiths singularity. Quenched disorder is independent of time, and it can take the form of oxygen vacancies or impurity atoms, or extended defects, etc. Although the properties (such as carrier density or T_c) of 2DEG at the LAO/STO interface can be tuned by applying a gate voltage, the impact of quenched

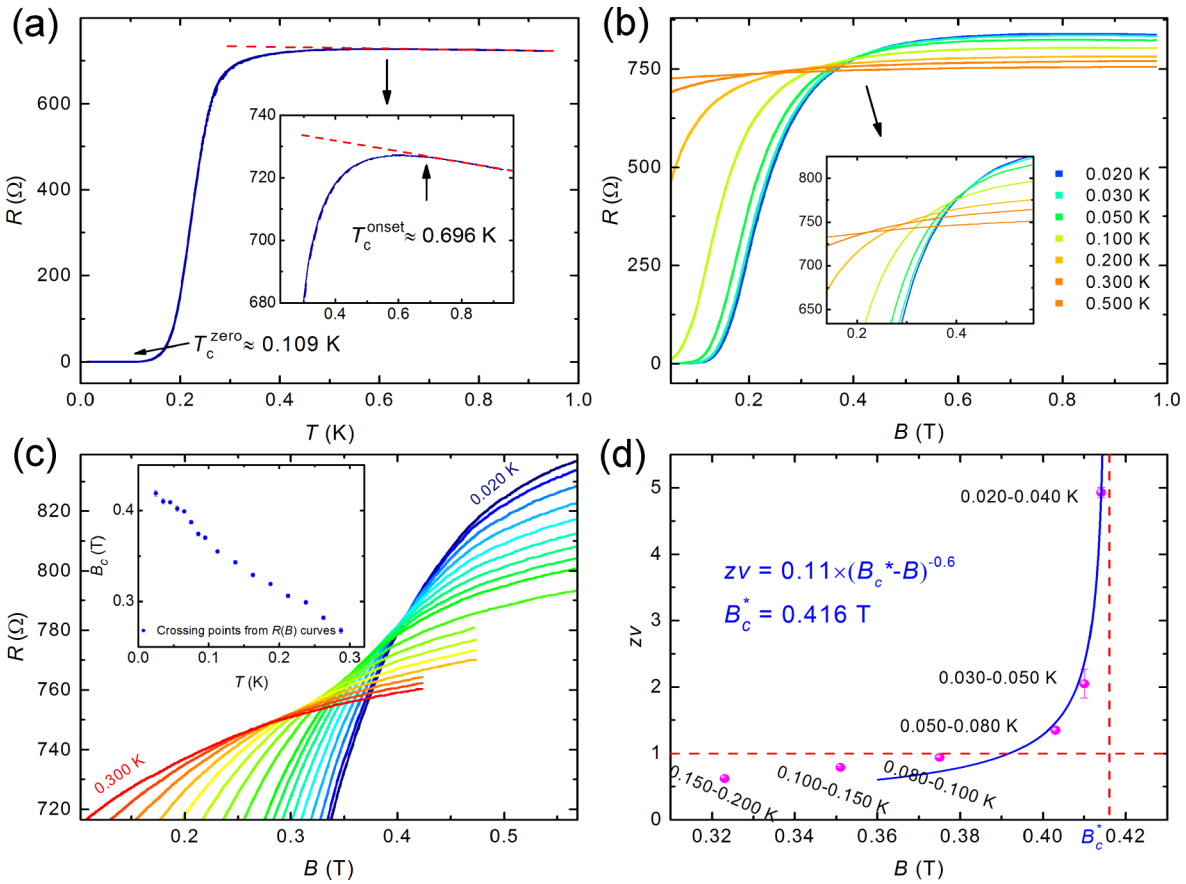

FIG. 5. The quantum Griffiths singularity for $V_G = 20$ V. (a) $R(T)$ at zero magnetic field with $T_c^{\text{zero}} = 0.109$ K. The inset shows the definition of T_c^{onset}, with a value of 0.696 K. (b) Isotherms $R(B)$ measured at different T. Zoom-in view of cross region is shown in the inset. (c) Isotherms $R(B)$ measured at different T ranging from 0.020 K to 0.300 K. The inset provides the crossing points B_c as a function of T, which were determined from the cross point of every two adjacent $R(B)$ curves. (d) The B dependence of zv values reveals the activated scaling behavior.

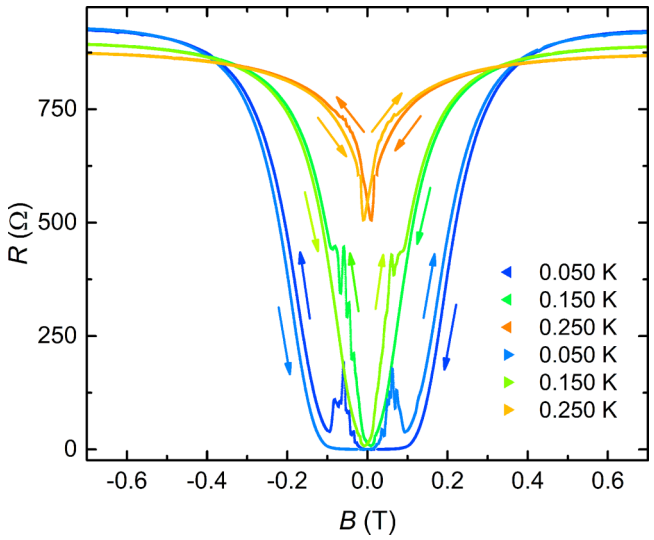

FIG. 6. The hysteretic behavior of $R(B)$ at different temperatures plotted for $V_G = 0$ V. The peaks that emerge in the magnetoresistance weaken with increasing temperature, while the corresponding magnetic field value remains unchanged. The arrows indicate the sweep directions of the magnetic field.

disorder on phase transitions still exists; thus, the quantum Griffiths singularity for different gate voltages can be observed. Also, compared to the state where $V_G = 0$ V, T_c decreases with increasing V_G, and the $z\nu$ value for the same temperature region becomes larger, which suggests that the influence of disorder on phase transition might be tuned by gate voltages.

The quenched disorder is normal in realistic low-dimensional systems and plays an important role in the destruction of the clean critical point [20,21]. From a statistical point of view, the influence of randomness on a clean critical point is determined by the trends of average disorder strength under coarse graining, known as the Harris criterion [35]. A recent theoretical work [36] has proposed that under certain conditions, if the clean critical point violates the Harris criterion, the magnitude of inhomogeneities increases without limit under coarse graining, and the dynamical exponent z diverges when approaching the disordered critical point. This prediction connects the violation of Harris criterion with the existence of a quantum Griffiths singularity and can apply to a variety of systems, including the quantum random transverse field Ising model [24,25,37]. In recent years, some experimental signatures related to the quantum Griffiths singularity have been reported in magnetic metals [38–43]. On the microscopic level, this quenched disorder introduces large rare regions, which can be locally ordered in one phase and further influence the scaling behavior. The above mentioned theoretical results can also be applied to SMT systems with clean critical exponent $\nu = 1/2$, in which the Harris criterion is certainly violated under quenched disorder [36,44].

For the SMT at the LAO/STO(110) interface, we find that the critical exponent $z\nu$ diverges at the ultralow-temperature limits, and we attribute such an unconventional quantum critical behavior to the effect of quenched disorder [20,21,24,25,45]. In the superconducting 2DEG at the LAO/STO(110) interface, there is a transition from a clean ($z\nu \leqslant 1$) to a dirty limit (Fig. 4). The scaling exponent $z\nu$ diverges rapidly upon approaching the QCP, which is consistent with the activated scaling behavior. When approaching the QCP, the effect of quenched disorder overtakes the thermal fluctuations and results in large local superconducting islands in which the dynamics are frozen. At low temperatures, these superconducting islands couple with each other via long-range Josephson coupling, and so global superconductivity emerges. At high temperatures, the thermal fluctuations smear the inhomogeneity induced by quenched disorder. In all, in accordance with theoretical expectation, our experimental observation suggests the SMT at the LAO/STO interface is of the infinite-randomness type.

Recently, direct evidence of the quantum Griffiths singularity was observed in a thin-film superconducting system [27]. In Ga film, an anomalous upturn of the upper "critical field" was observed when approaching zero temperature. However, for our LAO/STO interface, we did not observe the pronounced "tail" at ultralow temperatures (inset of Fig. 2). One possible reason for the absence of this extended phase boundary is due to the ultralow superconducting transition temperature of this interface superconductor, which is one order of magnitude lower than that of Ga film (~3.62 K). In Ga film, the temperature at which the critical exponent diverges is ultralow (~0.075 K) [27]. If simply comparing the results in the LAO/STO interface with that of Ga film, the pronounced "tail" should be expected to emerge at lower temperature (~0.025 K). In addition, the subtle nature or absence of an upturn might be attributed to the narrow range of temperature. Actually, a crossover-like behavior is observed at 0.030 K for our LAO/STO interface. However, the lowest electron temperature we had is 0.020 K. Hence, it is hard to observe the obvious extended phase boundary at the LAO/STO(110) interface. Also, the different disorder types in these two systems might also be responsible for the distinction in temperature dependence of "critical field".

Quantum criticality in magnetic-field-driven QPT has been studied previously at superconducting oxide interfaces, such as the $LaTiO_3/SrTiO_3(001)$ and LAO/STO(001) interfaces [12,46]. In the $LaTiO_3/SrTiO_3(001)$ interface, two different $z\nu$ values were obtained, and the observed critical behavior was single or double, depending on its conductance [46]. In LAO/STO(001) interface, a single $z\nu$ value was obtained that was independent of its conductance [12]. Here, however, we found a series of $z\nu$ values, independent of its conductance. In the low-temperature range, the $z\nu$ value is larger. With increasing temperature, the $z\nu$ value decreases. Moreover, we note that the resistance range of the crossing region only extends over a few tens of ohms. Thus, for lower conductance, the crossing region is hard to distinguish, as in Ref. [46]. Ultralow-temperature fine-resolution measurements are necessary to observe the Griffiths singularity in such interface superconducting systems.

Moreover, it is worth mentioning that the ferromagnetism was observed at the LAO/STO(110) interface. As shown in Fig. 6, when sweeping the field in both directions, hysteretic magnetoresistance is observed. The main peaks in the magnetoresistance appear at $B \approx \pm 0.06$ T and are weakened with increasing temperature. Also, less prominent peaks appear around main peaks. The hysteresis is reminiscent of the presence of ferromagnetism order, and

the additional peaks can be attributed to more complex magnetization dynamics [47]. Moreover, the amplitude of peaks decreases when decreasing the field sweep rate (Fig. 12 in the Appendix). Similar hysteretic magnetoresistance is observed at the superconducting LAO/STO(001) interfaces as the transport evidence for coexistence of superconductivity and ferromagnetism [5,47]. The measurements using a scanning superconducting quantum interference device [4] and magnetic torque magnetization [6] also showed evidence of the ferromagnetism at superconducting LAO/STO(001) interfaces. However, to our knowledge, at LAO/STO(110) interface, the coexistence of superconductivity and ferromagnetism has not been reported yet. In fact, one recent theoretical investigation predicted that ferromagnetism can appear in the (110) case too [48]. Our work provides experimental evidence of this theoretical prediction. Superconductivity and ferromagnetism are usually believed to be antagonistic phenomena. Two scenarios have been proposed to explain the coexistence of superconductivity and ferromagnetism at the LAO/STO(001) interface. One is the unconventional pairing mechanism, such as finite momentum pairing [49], through which a magnetic ordering and superconducting 2DEG is formed by the same electron system [50]. The other scenario is spatial phase separation, in which magnetism and superconductivity are generated by different electron layers [4,51]. Our current results cannot distinguish the mechanism(s) that induces the coexistence of superconductivity and ferromagnetism at the LAO/STO(110) interface. Since the (110) interface shows different orbital reconstruction compared with the (001) system [52], our observation offers a new platform in which to study superconductivity and ferromagnetism at the oxides interface. In addition, ferromagnetism might have influence on the rare regions (superconducting islands). It would be a very interesting topic to investigate both theoretically and experimentally whether or not the existence of ferromagnetism at the superconducting interface affects the observed quantum Griffiths singularity.

IV. CONCLUSION

In conclusion, we have shown a SMT in the superconducting 2DEG at the LAO/STO(110) interface. The diverging dynamic critical exponent is consistent with the quantum Griffiths singularity. The diverging dynamic critical exponent in the 2DEG provides new evidence of the quantum Griffiths singularity in addition to that in Ga thin film, hinting that different superconducting systems can be possibly treated within a uniform theoretical framework. Furthermore, our detection of hysteretic behavior indicates ferromagnetism at superconducting LAO/STO(110) interfaces.

ACKNOWLEDGMENTS

We thank Fa Wang and Limei Xu for helpful discussions. We acknowledge financial support from the National Basic Research Program of China (Grants No. 2013CB934600, No. 2012CB921300, No. 2013CB921701, No. 2013CBA01603, No. 2015CB921101, and No. 2014CB920903), the National Natural Science Foundation of China (Grants No. 11474022, No. 51172029, No. 11374035, No. 11274020, No. 11322435, and No. 11422430), and the Research Fund for the Doctoral Program of Higher Education (RFDP) of China. The Open Research Fund Program of the State Key Laboratory of Low-Dimensional Quantum Physics, Tsinghua University under Grant No. KF201501, and the Open Project Program of the Pulsed High Magnetic Field Facility (Grant No. PHMFF2015002), Huazhong University of Science and Technology.

S.S., Y.X., and P.W. contributed equally to this work.

APPENDIX

Here we provide the additional figures to supplement the main text.

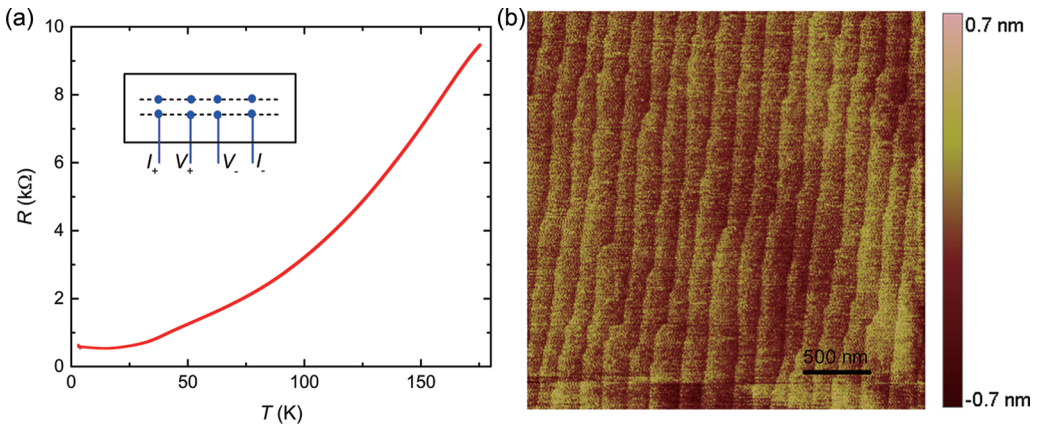

FIG. 7. (a) Typical resistance versus temperature curve measured for a low-temperature system (4–180 K). The inset shows the configuration of the electrodes for standard four-terminal measurements. (b) Atomic force microscopy surface topography of the 5 unit-cell LAO film. Atomically flat terraces were preserved after the film deposition.

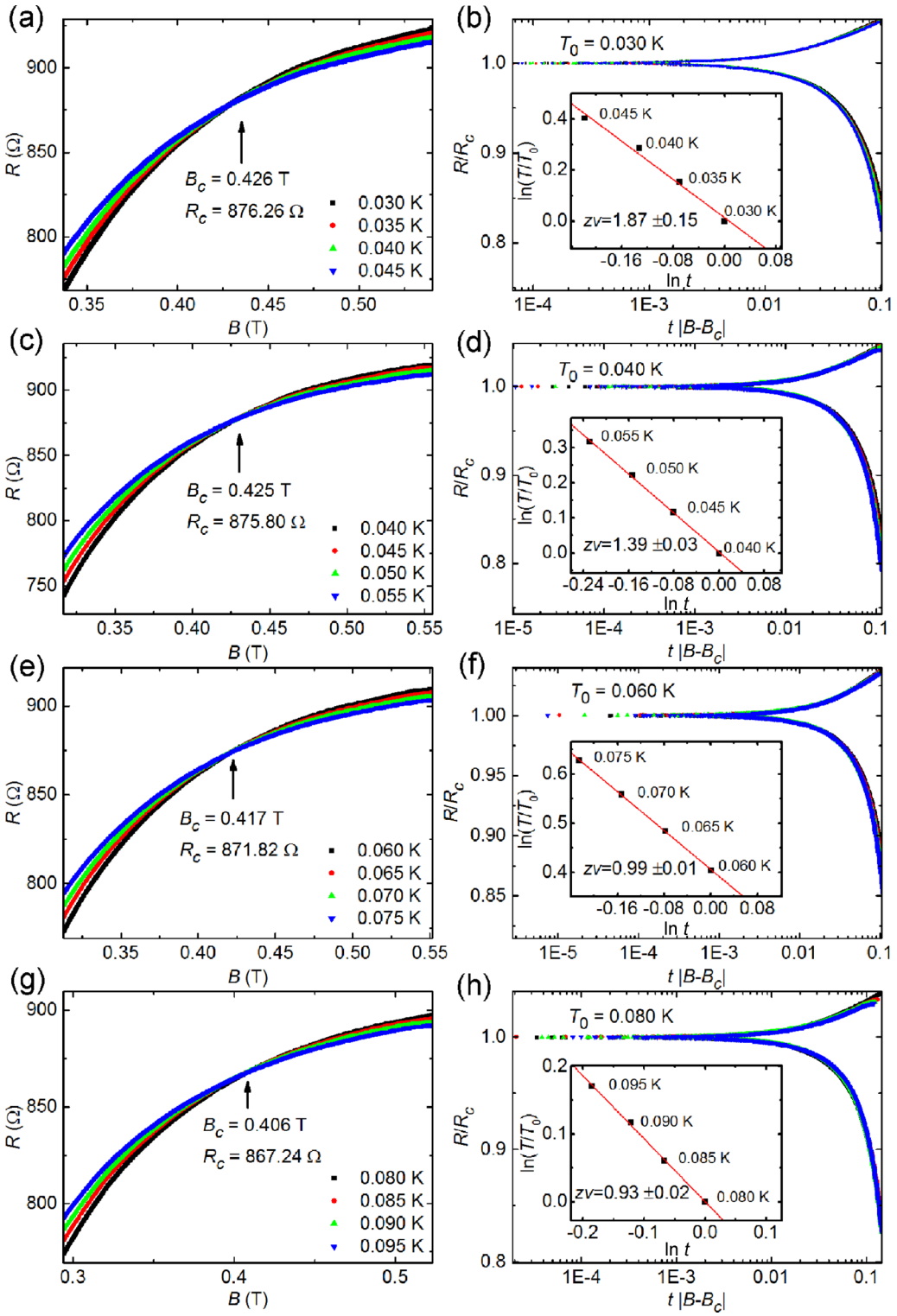

FIG. 8. Finite-size scaling analysis (0.020–0.0.95 K). (a), (c), (e), (g) Isotherms $R(B)$ close to the critical points at different temperature regions. The crossing region formed by four adjacent $R(B)$ curves is denoted as one critical point. (b), (d), (f), (h) Normalized R as a function of $t|B_c - B|$, where $t = (T/T_0)^{-1/z\nu}$. The insets show the power-law plot T dependence of scaling parameter t. The linear fitting gives the $z\nu$ values.

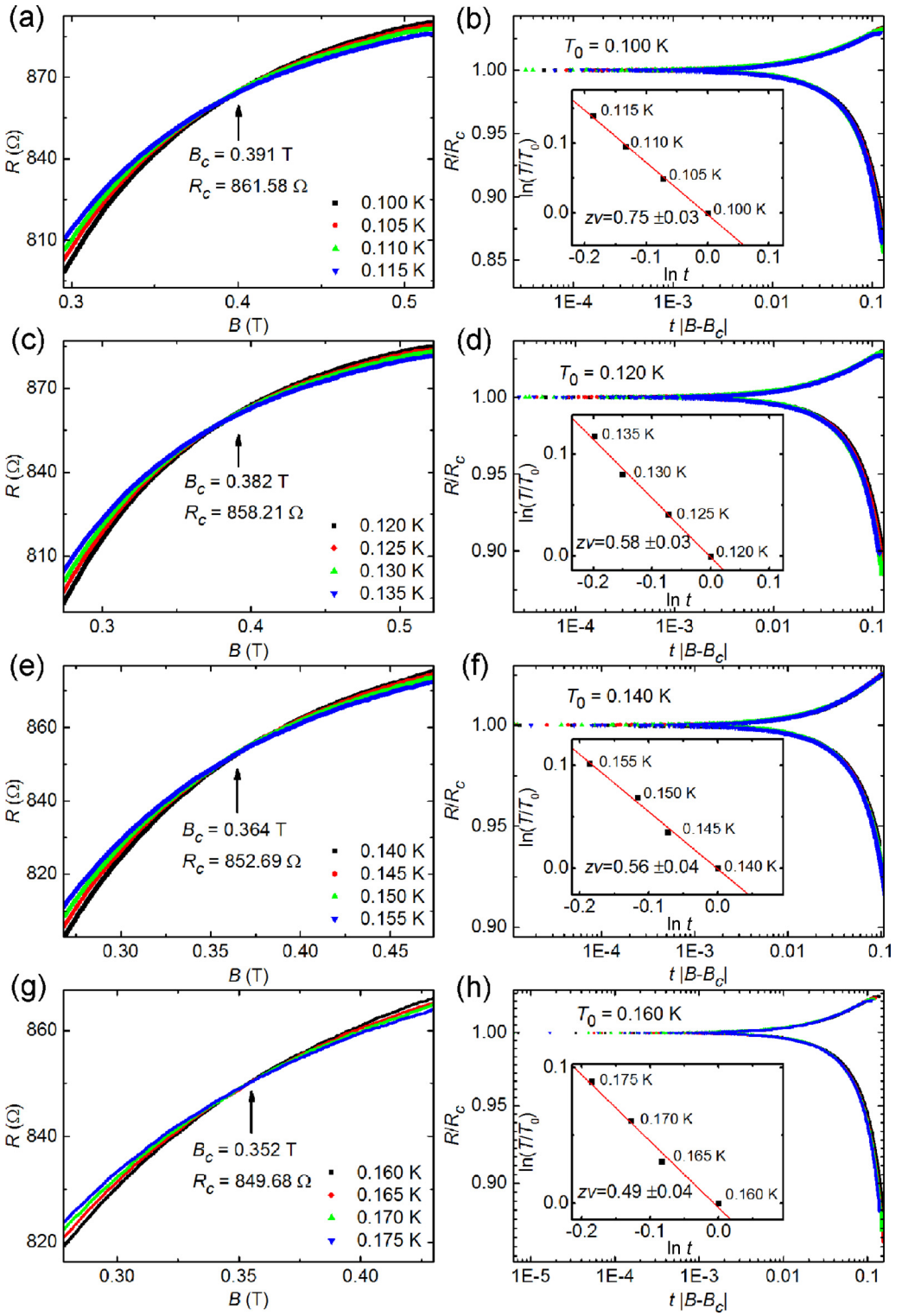

FIG. 9. Finite-size scaling analysis (0.100–0.0.175 K). (a), (c), (e), (g) Isotherms $R(B)$ close to the critical points at different temperature regions. (b), (d), (f), (h) Normalized R as a function of $t|B_c - B|$, where $t = (T/T_0)^{-1/zv}$. The insets show the power-law plot T dependence of scaling parameter t. The zv values are obtained from the slope of the fitting line.

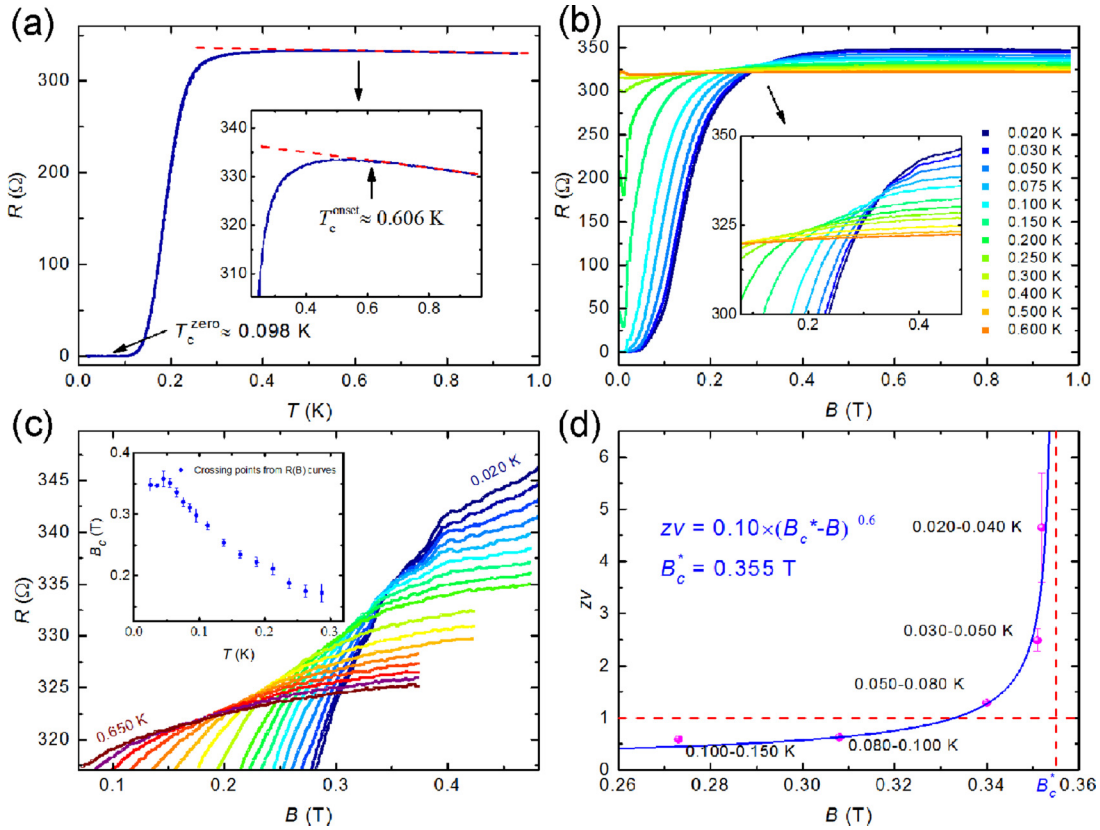

FIG. 10. The quantum Griffiths singularity for $V_G = 60$ V. (a) $R(T)$ at zero magnetic field gives $T_c^{\rm zero} \approx 0.098$ K, and the inset shows the definition of $T_c^{\rm onset}$, with a value of 0.696 K. The temperature where the $R(T)$ first deviates from its linear dependence at high temperature is defined as $T_c^{\rm onset}$. (b) Isotherms $R(B)$ measured at different T. Close-up view of cross region is shown in the inset. (c) Isotherms $R(B)$ measured in detail at different T ranging from 0.020 K to 0.650 K. The inset gives the crossing points B_c as a function of T, which are formed by every two adjacent $R(B)$ curves. (d) The B dependence of zv values gives the activated scaling behavior. As we can see, the critical exponent diverges at low temperatures. Thus, the quantum Griffiths singularity is also observed for $V_G = 60$ V.

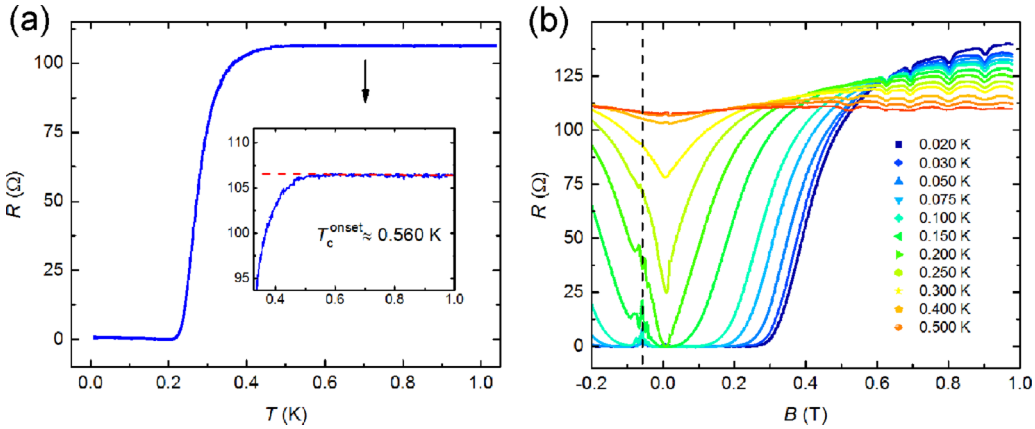

FIG. 11. The measurements of the 12-unit-cell LAO/STO(110) sample prepared under the same conditions as the 5-unit-cell sample (the main text). (a) $R(T)$ at zero magnetic field with $T_c^{\rm onset} \approx 0.560$ K. (b) Isotherms $R(B)$ measured at different T. The crossing region around 0.530 T is formed instead of one crossing point, which is analogous to data from the 5-unit-cell sample. The periodic oscillation of the normal state resistance is somewhat puzzling. We speculate that it may be due to the accidental formation of conducting loops at the interface. The magnetoresistance peaks also appear at around -0.056 T, as marked by the dashed line. The magnetic field sweeps from positive to negative.

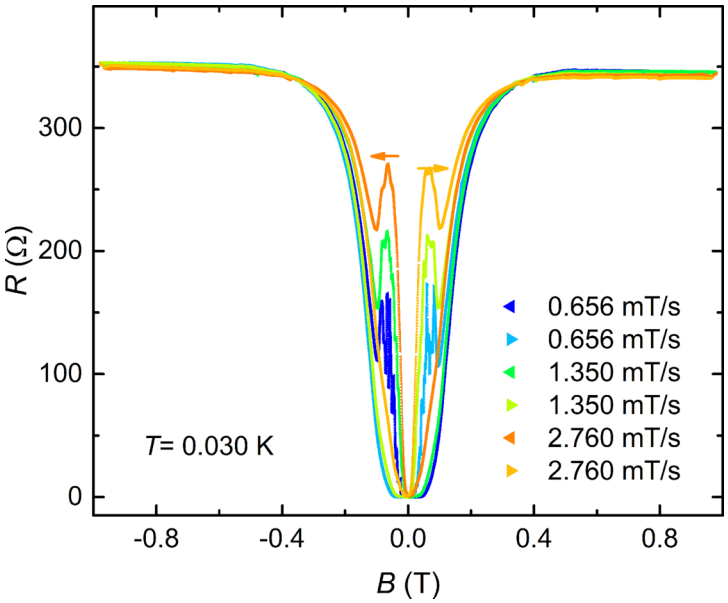

FIG. 12. The hysteretic behavior of $R(B)$ with different sweep rate of the magnetic field at $T = 0.030\,\mathrm{K}$ for $V_G = 60\,\mathrm{V}$. The amplitude of the peak increases when the field sweep rate increases. The arrows indicate the sweep direction of the magnetic field. The arrow pointing left indicates the magnetic field sweeps from positive to negative, while the arrow pointing right shows the opposite. Similar results have been reported at LAO/STO(001) interfaces [47]. The property of the $R(B)$ curves suggests the coexistence of superconductivity and ferromagnetism at the LAO/STO(110) interfaces.

[1] A. Ohtomo and H. Y. Hwang, Nature **427**, 423 (2004).
[2] N. Reyren, S. Thiel, A. D. Caviglia, L. Fitting Kourkoutis, G. Hammerl, C. Richter, C. W. Schneider, T. Kopp, A.-S. Rüetschi, D. Jaccard, M. Gabay, D. A. Muller, J.-M. Triscone, and J. Mannhart, Science **317**, 1196 (2007).
[3] A. Brinkman, M. Huijben, M. van Zalk, J. Huijben, U. Zeitler, J. C. Maan, W. G. van der Wiel, G. Rijnders, D. H. A. Blank, and H. Hilgenkamp, Nat. Mater. **6**, 493 (2007).
[4] J. A. Bert, B. Kalisky, C. Bell, M. Kim, Y. Hikita, H. Y. Hwang, and K. A. Moler, Nat. Phys. **7**, 767 (2011).
[5] D. A. Dikin, M. Mehta, C. W. Bark, C. M. Folkman, C. B. Eom, and V. Chandrasekhar, Phys. Rev. Lett. **107**, 056802 (2011).
[6] L. Li, C. Richter, J. Mannhart, and R. C. Ashoori, Nat. Phys. **7**, 762 (2011).
[7] K. Klitzing, G. Dorda, and M. Pepper, Phys. Rev. Lett. **45**, 494 (1980).
[8] R. B. Laughlin, Phys. Rev. Lett. **50**, 1395 (1983).
[9] D. C. Tsui, H. L. Stormer, and A. C. Gossard, Phys. Rev. Lett. **48**, 1559 (1982).
[10] H. L. Stormer, Rev. Mod. Phys. **71**, 875 (1999).
[11] A. D. Caviglia, S. Gariglio, N. Reyren, D. Jaccard, T. Schneider, M. Gabay, S. Thiel, G. Hammerl, J. Mannhart, and J.-M. Triscone, Nature **456**, 624 (2008).
[12] M. M. Mehta, D. A. Dikin, C. W. Bark, S. Ryu, C. M. Folkman, C. B. Eom, and V. Chandrasekhar, Phys. Rev. B **90**, 100506(R) (2014).
[13] G. Herranz, F. Sanchez, N. Dix, M. Scigaj, and J. Fontcuberta, Sci. Rep. **2**, 758 (2012).
[14] Y.-L. Han, S.-C. Shen, J. You, H.-O. Li, Z.-Z. Luo, C.-J. Li, G.-L. Qu, C.-M. Xiong, R.-F. Dou, L. He, D. Naugle, G.-P. Guo, and J.-C. Nie, Appl. Phys. Lett. **105**, 192603 (2014).
[15] G. Herranz, G. Singh, N. Bergeal, A. Jouan, J. Lesueur, J. Gázquez, M. Varela, M. Scigaj, N. Dix, F. Sánchez, and J. Fontcuberta, Nat. Commun. **6**, 6028 (2015).
[16] M. B. Salamon and S. H. Chun, Phys. Rev. B **68**, 014411 (2003).
[17] V. M. Galitski, A. Kaminski, and S. Das Sarma, Phys. Rev. Lett. **92**, 177203 (2004).
[18] P. Y. Chan, N. Goldenfeld, and M. Salamon, Phys. Rev. Lett. **97**, 137201 (2006).
[19] R. B. Griffiths, Phys. Rev. Lett. **23**, 17 (1969).
[20] T. Vojta, J. Phys. A-Math. Gen. **39**, R143 (2006).
[21] T. Vojta, J. Low Temp. Phys. **161**, 299 (2010).
[22] A. Del Maestro, B. Rosenow, J. A. Hoyos, and T. Vojta, Phys. Rev. Lett. **105**, 145702 (2010).
[23] B. M. McCoy, Phys. Rev. Lett. **23**, 383 (1969).
[24] D. S. Fisher, Phys. Rev. Lett. **69**, 534 (1992).
[25] D. S. Fisher, Phys. Rev. B **51**, 6411 (1995).
[26] M. Brando, D. Belitz, F. M. Grosche, and T. R. Kirkpatrick, Rev. Mod. Phys. **88**, 025006 (2016).
[27] Y. Xing, H.-M. Zhang, H.-L. Fu, H. Liu, Y. Sun, J.-P. Peng, F. Wang, X. Lin, X.-C. Ma, Q.-K. Xue, J. Wang, and X. C. Xie, Science **350**, 542 (2015).
[28] N. Markovic, Science **350**, 509 (2015).
[29] M. P. A. Fisher, Phys. Rev. Lett. **65**, 923 (1990).
[30] A. Goldman, Int. J. Mod. Phys. B **24**, 4081 (2010).
[31] S. L. Sondhi, S. M. Girvin, J. P. Carini, and D. Shahar, Rev. Mod. Phys. **69**, 315 (1997).
[32] N. Mason and A. Kapitulnik, Phys. Rev. B **64**, 060504 (2001).
[33] T. Vojta, A. Farquhar, and J. Mast, Phys. Rev. E **79**, 011111 (2009).
[34] I. A. Kovács and F. Iglói, Phys. Rev. B **82**, 054437 (2010).
[35] A. B. Harris, J. Phys. C: Solid State Phys. **7**, 1671 (1974).
[36] T. Vojta and J. A. Hoyos, Phys. Rev. Lett. **112**, 075702 (2014).
[37] O. Motrunich, S. C. Mau, D. A. Huse, and D. S. Fisher, Phys. Rev. B **61**, 1160 (2000).
[38] C. L. Seaman, M. B. Maple, B. W. Lee, S. Ghamaty, M. S. Torikachvili, J.-S. Kang, L. Z. Liu, J. W. Allen, and D. L. Cox, Phys. Rev. Lett. **67**, 2882 (1991).
[39] M. C. de Andrade, R. Chau, R. P. Dickey, N. R. Dilley, E. J. Freeman, D. A. Gajewski, M. B. Maple, R. Movshovich,

A. H. Castro Neto, G. Castilla, and B. A. Jones, Phys. Rev. Lett. **81**, 5620 (1998).
[40] S. Guo, D. P. Young, R. T. Macaluso, D. A. Browne, N. L. Henderson, J. Y. Chan, L. L. Henry, and J. F. DiTusa, Phys. Rev. Lett. **100**, 017209 (2008).
[41] J. G. Sereni, T. Westerkamp, R. Küchler, N. Caroca-Canales, P. Gegenwart, and C. Geibel, Phys. Rev. B **75**, 024432 (2007).
[42] T. Westerkamp, M. Deppe, R. Kuchler, M. Brando, C. Geibel, P. Gegenwart, A. P. Pikul, and F. Steglich, Phys. Rev. Lett. **102**, 206404 (2009).
[43] S. Ubaid-Kassis, T. Vojta, and A. Schroeder, Phys. Rev. Lett. **104**, 066402 (2010).
[44] S. Sachdev, P. Werner, and M. Troyer, Phys. Rev. Lett. **92**, 237003 (2004).
[45] D. S. Fisher, M. P. A. Fisher, and D. A. Huse, Phys. Rev. B **43**, 130 (1991).
[46] J. Biscaras, N. Bergeal, S. Hurand, C. Feuillet-Palma, A. Rastogi, R. C. Budhani, M. Grilli, S. Caprara, and J. Lesueur, Nat. Mater. **12**, 542 (2013).
[47] M. M. Mehta, D. A. Dikin, C. W. Bark, S. Ryu, C. M. Folkman, C. B. Eom, and V. Chandrasekhar, Nat. Commun. **3**, 955 (2012).
[48] G. Chen and L. Balents, Phys. Rev. Lett. **110**, 206401 (2013).
[49] K. Michaeli, A. C. Potter, and P. A. Lee, Phys. Rev. Lett. **108**, 117003 (2012).
[50] M. S. Scheurer and J. Schmalian, Nat. Commun. **6**, 6005 (2015).
[51] S. Banerjee, O. Erten, and M. Randeria, Nat. Phys. **9**, 625 (2013).
[52] D. Pesquera, M. Scigaj, P. Gargiani, A. Barla, J. Herrero-Martín, E. Pellegrin, S. M. Valvidares, J. Gázquez, M. Varela, N. Dix, J. Fontcuberta, F. Sánchez, and G. Herranz, Phys. Rev. Lett. **113**, 156802 (2014).